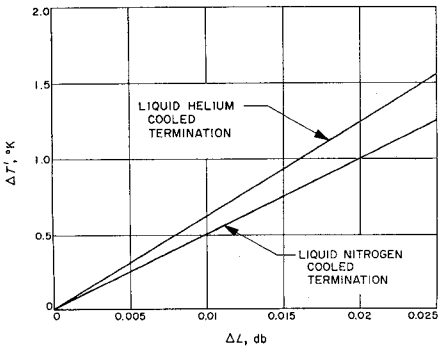

Fig. 2. Calibration error in a reference termination due to insertion-loss measurement error.

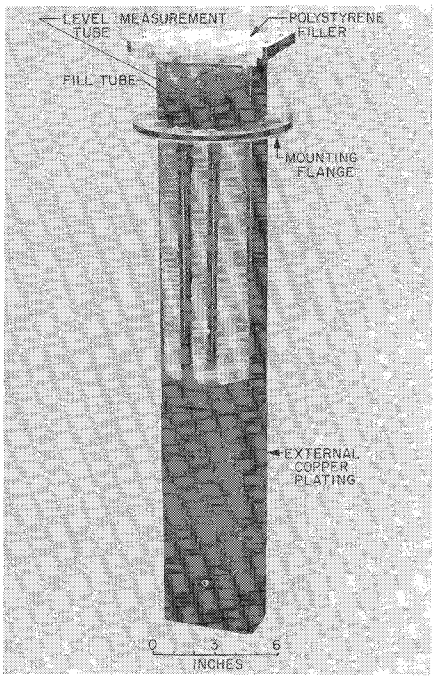

Fig. 3. *S*-band WR-430 waveguide liquid-helium-cooled termination.

ation requires better than 0.002-dB accuracy in the insertion-loss measurements [8].

Experimental Calibrated Thermal Termination

An *S*-band (Fig. 3) waveguide liquid-helium-cooled thermal termination [3] was calibrated to high precision using (11). Waveguide construction was used to minimize losses. This termination is normally installed in a 10-liter-glass Dewar, and has about 10 hours of operating life. The stainless-steel section of copper-plated waveguide located between the external copper-plated section containing the cooled termination and the mounting flange had an insertion loss of L_1 of 0.009 dB. The outer section of waveguide above the mounting flange had at ambient temperature an insertion loss L_2 of 0.008 dB. (This includes the polystyrene waveguide window.) With reference to the input flange, the equivalent noise temperature is 5.0°K [from (11)] over the frequency ranges where the termination is matched. An accuracy of 10 per cent in the calibration of the transmission line would result in less than 0.1°K error in the equivalent noise temperature.

C. T. Stelzried
Telecommunications Div.
Jet Propulsion Lab.
California Institute of Technology
Pasadena, Calif.

References

[1] Schuster, D., C. T. Stelzried, and G. S. Levy, The determination of noise temperatures of large paraboloidal antennas, *IRE Trans. on Antennas and Propagation*, vol AP-10, May 1962, pp 286–291.
[2] Stelzried, C. T., A liquid-helium-cooled coaxial termination *Proc. IRE*, (*Correspondence*), vol 49, Jul 1961, p. 1224.
[3] Clauss, R. C., W. Higa, C. Stelzried, and E. Wiebe, Total system noise temperature: 15°K, *IEEE Trans. on Microwave Theory and Techniques*, (*Correspondence*), vol MTT-12, Nov 1964, pp 619–620.
[4] Beatty, R. W., Mismatch errors in the measurement of ultra high frequency and microwave variable attenuations, *J. Res. Nat. Bur. Std.*, vol 52, no. 1, Res. Paper 2465, 1954.
[5] Daywitt, W. C., Microwave noise, in *National Bureau of Standards Course on Electromagnetic Measurements and Standards*. Boulder, Colo.: U. S. Dept. of Commerce, Jul 1963.
[6] Siegman, A. E., Thermal noise in microwave systems, *Microwave J.*, Mar 1961.
[7] Ford, L. R., *Differential Equations*, 2nd ed., New York: McGraw-Hill, 1955.
[8] Stelzried, C. T., and S. M. Petty, Microwave insertion loss test set, *IEEE Trans. on Microwave Theory and Techniques*, (*Correspondence*), vol MTT-12, Jul 1964, pp 475–477.

Graphical Procedures for Finding Matrix Elements for a Lattice Network and a Section of Transmission Line

Four-terminal networks and two-port junctions can be represented by several different well-known 2 by 2 matrices. Tables relating the elements in the various matrices have been published.[1–5] Graphical procedures are presented here which may be used to determine the elements in these matrices for a lattice network and a section of transmission line, as shown in Fig. 1.

In the discussion which follows,

$$\Gamma(Z) = (Z-1)/(Z+1)$$

and

$$Z(\Gamma) = (1+\Gamma)/(1-\Gamma)$$

Derivations are omitted because they are simply boring algebraic manipulations.

The elements of the scattering matrix for a lattice network are given by

$$2S_{11} = 2S_{22} = \Gamma(Z_a') + \Gamma(Z_b')$$
$$2S_{12} = 2S_{21} = -\Gamma(Z_a') + \Gamma(Z_b')$$

Manuscript received July 13, 1964; revised September 28, 1964.

[1] Guillemin, E. A., *Communication Networks*, vol II. New York: John Wiley, 1935, pp 137–138.
[2] Bolinder, E. F., Note on the matrix representation of linear two-port networks, *IRE Trans. on Circuit Theory*, vol CT-4, Dec 1957, pp 337–339.
[3] Beatty, R. W., and D. M. Kerns, Relationships between different kinds of network parameters, not assuming reciprocity or equality of the waveguide or transmission line characteristic impedances, *Proc. IEEE*, vol 52, Jan 1964, p 84.
[4] Mathis, H. F., Matrix conversion table, *Microwaves*, vol 3, Feb 1964, pp 28–33.
[5] Kopp, E. H., Matrices for basic two-port networks, *Electro-Technology*, vol 73, Mar 1964, pp 34–39.

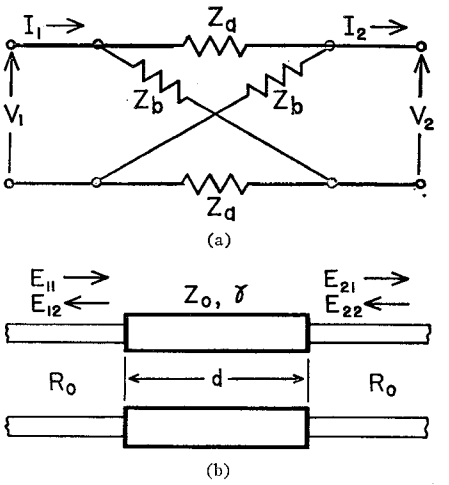

Fig. 1. The two networks considered.

where it is assumed that two transmission lines with characteristic impedance R_0 are connected to the network, $Z_a' = Z_a/R_0$, and $Z_b' = Z_b/R_0$. A graphic method for finding these elements is illustrated in Fig. 2, and either a Smith or a Carter chart[6,7] may be used.

Logarithmic transmission-line charts[8–10] are used to find the matrix elements for a section of transmission line and a lattice network. The following points are located on the chart, as shown in Fig. 3: E at the left $Z = \infty$, F at $Z = 0$, G at $Z = 1 \angle -90° = -j$, and H at the right $Z = \infty$. The points J and K are plotted at $Z_J = R_0/Z_0$, and $Z_K = Z_0/R_0 = 1/Z_J$. The point L is located so that $(\overline{EL})/(\overline{EH}) = \alpha/2\beta$, where $\gamma = \alpha + j\beta$. The point M is located on the line LH at the horizontal distance $d/\lambda_g = \beta d/2\pi$ from H as shown. The point N is the midpoint of the line MH. For a lattice network,

$$Z_K = \sqrt{Z_a Z_b'} = \sqrt{Z_a Z_b}/R_0$$
$$Z_N = \sqrt{Z_b'/Z_a'} = \sqrt{Z_b/Z_a}$$

and

$$Z_0 = \sqrt{Z_a Z_b}$$

The point P is located on the line HJ so that $\overline{JP} = \overline{HJ}$. The point Q is located on the line FK so that $\overline{KQ} = \overline{FK}$. The lines RG, KS, UJ, QW, and XP are drawn parallel to the line LH. The various points are located so that

$$\overline{RG} = \overline{MN} = \overline{NH} = \overline{KS} = \overline{UV} = \overline{VJ} = \overline{QW} = \overline{XP}$$

and

$$\overline{MU} = \overline{FK} = \overline{KQ} = \overline{NV} = \overline{V\bar{X}} = \overline{SW} = \overline{HJ} = \overline{JP}$$

[6] Smith, P. H., Transmission-line calculator, *Electronics*, vol 12, Jan 1939, pp 29–31; An improved transmission-line calculator, vol 17, Jan 1944, pp 130–133, 318, 320, 322, 324, 325.
[7] Carter, P. S., Charts for transmission line measurements and computations, *RCA Rev*, vol 3, Jan 1939, pp 355–368.
[8] Cafferata, H., The calculation of input impedance, or sending-end impedance of feeders and cables terminated by complex loads, *Marconi Rev.*, no. 64, Jan–Feb 1937, pp 12–19; no. 67, Sep–Dec 1937, pp 21–39.
[9] Guillien, R., Nouveau diagramme permettant par translation les transformations d'impedances, *L'Onde Electrique*, vol 35, Dec 1955, pp 1164–1170.
[10] Mathis, H. F., Logarithmic transmission-line charts, *Electronics*, vol 34, Dec 1, 1961, pp 48, 50, 52, 54.

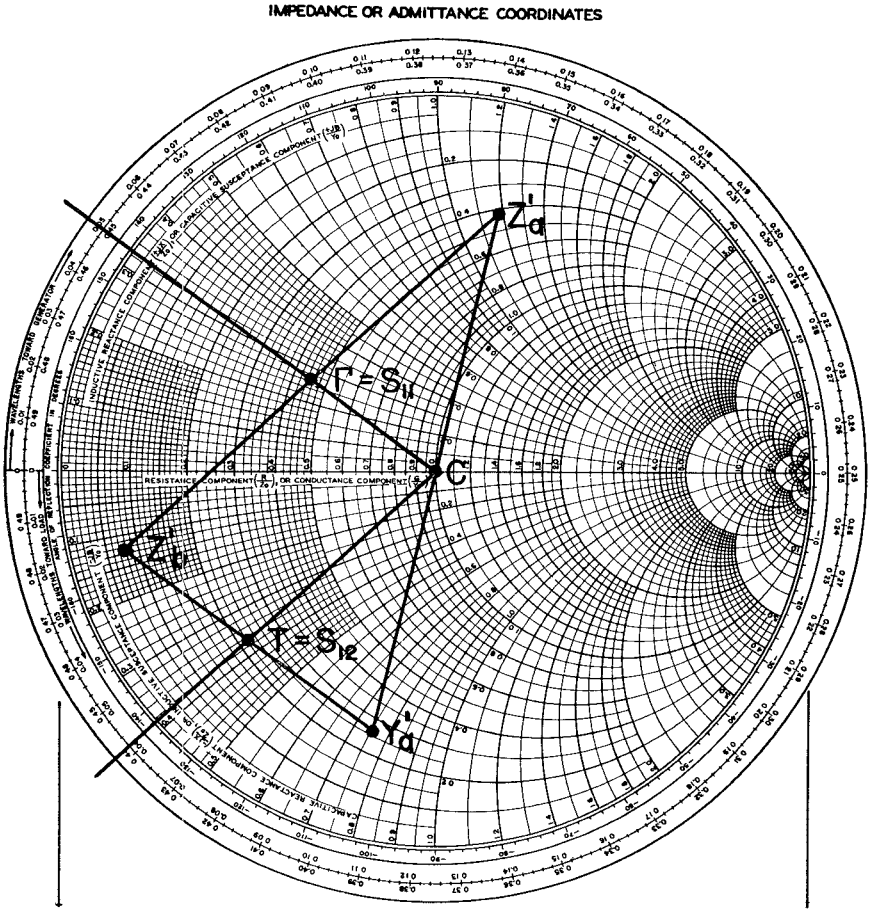

Fig. 2. Construction for finding S_{11} and S_{12} for a lattice network, by using a circular transmission-line chart.

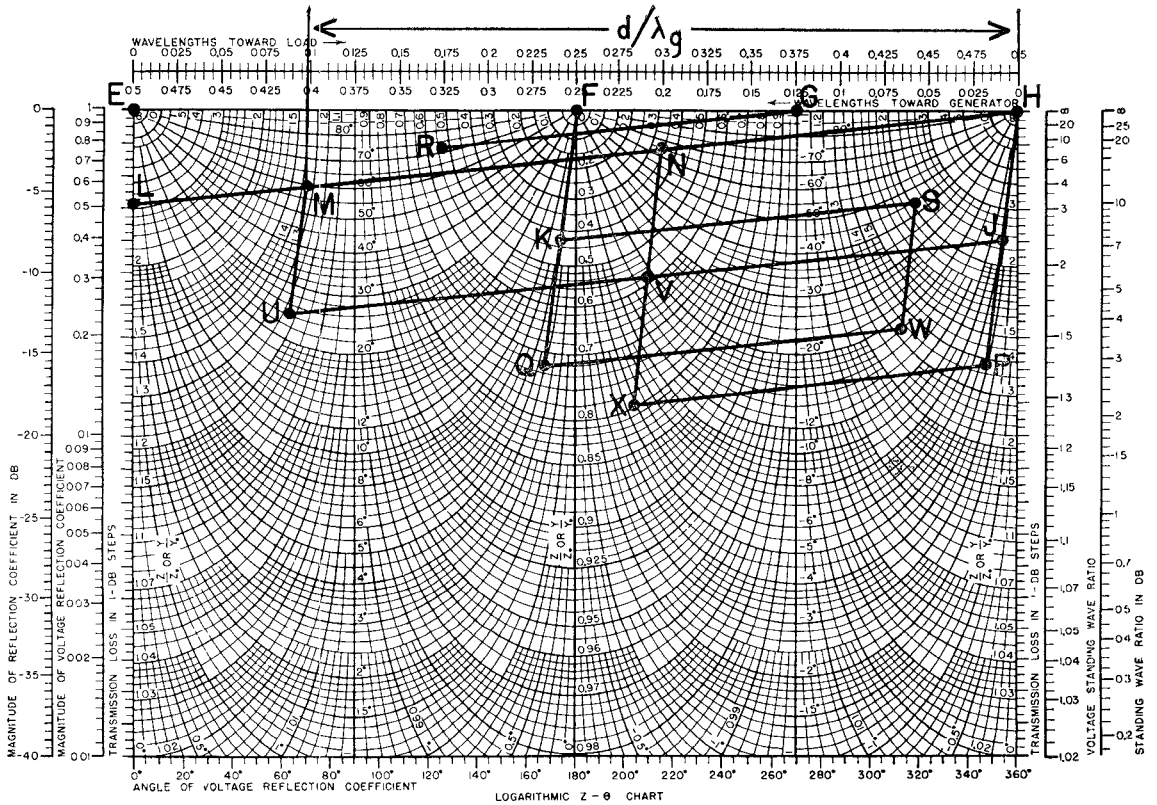

Fig. 3. Construction for finding matrix elements, by using a logarithmic transmission-line chart.

Let k and $\sigma = \exp(-\gamma d)$ denote the voltage reflection coefficients corresponding to Z_K and Z_N, respectively. The voltage reflection coefficients for all points are simple functions of k and σ.

In some cases, the matrix element is found by determining the impedance Z corresponding to the element as a voltage reflection coefficient Γ. The impedance is plotted on a transmission-line chart, and the value of Γ is read off the chart to obtain the desired matrix element. If the impedance has a negative real component, or an angle outside the $-90°$ to $+90°$ range, an extended transmission-line chart[11] may be used. Since extended charts are not readily available, a conventional chart may be used by recalling that $Z(1/\Gamma) = -Z(\Gamma)$. One plots $-Z$, reads $c = 1/\Gamma$, and computes $\Gamma = 1/c$.

The elements of the Z matrix are given by

$$Z_{11} = Z_{22} = Z_0 \coth \gamma d = Z_0 Z(\sigma^2) = Z_0 Z_M$$

$$Z_{12} = Z_{21} = Z_0 / \sinh \gamma d$$

The term $\sinh \gamma d$, which appears in other matrix elements, is given by

$$Z(j \sinh \gamma d) = -[Z(-j\sigma)]^2 = -Z_R^2$$

The elements of the matrix are given by

$$Y_{11} = Y_{22} = \coth \gamma d / Z_0 = Z_M / Z_0$$

$$Y_{12} = Y_{21} = 1/Z_0 \sinh \gamma d$$

The elements of the $ABCD$ matrix are given by

$$Z(A) = Z(D) = \cosh \gamma d = -[Z(\sigma)]^2 = -Z_N^2$$

$$B = Z_0 \sinh \gamma d$$

$$C = \sinh \gamma d / Z_0$$

The scattering matrix elements are given by

$$Z(S_{11}) = Z(S_{22}) = Z(k)/Z(k\sigma^2) = Z_K Z_U = Z_U / Z_J$$

and

$$Z(S_{12}) = Z(S_{21}) = Z(\sigma)/Z(k^2\sigma) = Z_N / Z_X$$

The less known r matrix is defined by

$$\begin{pmatrix} E_{12} \\ E_{11} \end{pmatrix} = \begin{pmatrix} r_{11} & r_{12} \\ r_{21} & r_{22} \end{pmatrix} \begin{pmatrix} E_{22} \\ E_{21} \end{pmatrix}$$

The elements of this matrix are given by

$$Z(r_{11}) = Z(\sigma)/Z(k^2/\sigma) = Z_N Z_W$$

$$Z(r_{12}) = Z(-k\sigma)Z(k/\sigma) = Z_V Z_S$$

$$r_{21} = -r_{12}$$

$$Z(r_{22}) = -Z(\sigma)/Z(k^2\sigma) = -Z_N / Z_X$$

H. F. MATHIS
Dept. of Elec. Engrg.
The Ohio State University
Columbus, Ohio

[11] Mathis, H. F., Extended transmission-line charts, *Electronics*, vol 33, Sep 23, 1960, pp 76, 78.

Note on Tetrahedral Junction

Weiss [1] has described a reactive waveguide switch consisting of a ferrite rod at the junction of two mutually cross-polarized rectangular waveguides, as shown in Fig. 1. When the ferrite rod is unmagnetized, the system represents a transition to cutoff waveguide. When the ferrite rod is longitudinally magnetized, the RF energy is coupled to the crossed waveguide.

Weiss [2] has noted that the modes of propagation on the tetrahedral junction are the same as those on the Reggia and Spencer phase shifter [3]. He has described the useful operating range of these devices as extending from the onset of the dielectric waveguide effect to the onset of elliptical Faraday rotation. In this range, the Weiss model indicates that the composite ferrite air waveguide can support only a single elliptically polarized mode of propagation. As the ferrite rod is increased above a critical diameter, a second ellipitically polarized mode becomes propagating and the system exhibits elliptical Faraday rotation, that is, rotation is suppressed in the range of ferrite diameters for which only a single elliptically polarized mode is propagating.

It is the purpose of this note to describe the tetrahedral junction in terms of the single-tapered mode coupler. However, we shall first briefly compare mode interference couplers with those that are single tapered.

Miller [4] has shown that when two transmission lines with equal-phase velocities are continuously coupled over some length, power introduced into one line will be completely transferred periodically back and forth between them. Such a system can generally support two forward modes of propagation, which have equal amounts of power in each line and which propagate with different velocities through the structure. One is called the even mode, because the electric field is in the same direction in each line; the other is called the odd mode, because the fields are oppositely oriented. Power transfer is effected by the interference between these modes, and this type of coupler is therefore known as a mode interference coupler; in general, it is frequency dependent. This is what occurs in Faraday structures where the normal modes are circularly polarized. If power is introduced into both lines to correspond to one of the normal modes, no coupling will take place and the power will be emergent in the same normal mode. If the two coupled modes have a fixed-phase difference between them, the power transfer is still periodic, but now the normal modes have unequal powers in the two lines and the power division is dependent on the ratio of velocity difference to coupling factor.

More recently Cook [5] has shown that if the phase velocity difference between the two coupled lines is made grossly different at one end of the coupled lines, equal in the center, and again unequal in the opposite sense, complete power transfer with only a residual power fluctuation is effected, which, moreover, is independent of coupling factor and frequency, provided the coupling length is long. When this is so, excitation of one of the coupled lines corresponds to all the power in one of the forward normal modes of propagation, and the power division is simply dependent on the final-phase difference between the coupled lines. In such a system, one of the normal modes of propagation is discriminated against, and power transfer between the coupled lines occurs with only a single forward normal mode of propagation.

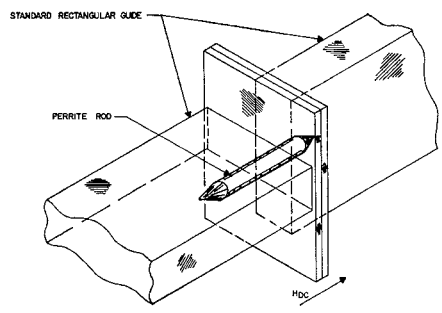

Fig. 1. The tetrahedral junction.

Fox [6] has enlarged on Cook's scheme and has shown that by varying both the velocities of the coupled lines and the coupling factor, the residual power fluctuation is eliminated. In particular, the difference in phase velocity is made to vary cosinusoidally and the coupling factor sinusoidally.

In mode interference couplers, the phase relation between the electric fields in the two lines is 90°. However, for this medium, the phase difference is 0° or 180°, depending on whether the power is introduced in the line having the higher or lower phase velocity; hence the coupled modes are the normal modes for the local cross section.

In the switch described by Weiss, the system represents a transition to cutoff waveguide when the ferrite is unmagnetized. At the plane of symmetry, the waveguide boundary conditions impose a sharp crossover of the phase velocities of the coupled modes. When the ferrite rod is magnetized, this phase distribution corresponds to a zero-dB coupler and the energy is accepted by the rotated waveguide. We also note that the wave is circularly polarized at the plane of symmetry.

Because the phase transition between the coupled modes is discontinuous, both normal modes are excited. However, one of these is cut off; hence no beat interference results. If at the same time the backward propagating mode is matched out, the power is transmitted past the junction.

More generally, the tetrahedral junction is only one example of several zero-dB couplers that rely on the single-tapered mode coupling theory in which one of the normal modes is cut off.

A second example was realized by taking an X-band 3-dB sidewall hybrid and placing metal inserts into the coupling region, as shown in Fig. 2. In this manner the TE_{20} mode, which is one of the normal modes of the hybrid, was cut off. The insertion loss for this structure between ports 1 and 2 was

Manuscript received October 2, 1964.